www.sciencemag.org/cgi/content/full/322/5899/246/DC1

Supporting Online Material for

Implications of Magma Transfer Between Multiple Reservoirs on Eruption Cycling

Derek Elsworth,* Glen Mattioli, Joshua Taron, Barry Voight, Richard Herd

*To whom correspondence should be addressed. E-mail: elsworth@psu.edu

Published 10 October 2008, *Science* **322**, 246 (2008)
DOI: 10.1126/science.1161297

This PDF file includes:

Supplementary Online Materials

Implications of Magma Transfer between Multiple Reservoirs on Eruption Cycling

Derek Elsworth,[1] Glen Mattioli,[2] Joshua Taron,[1] Barry Voight[1] and Richard Herd[3]

Methods

The history of magma exchange within the deep subsurface plumbing of volcanic systems may be recovered if both the surface efflux of magma and measured deformation of the surface are available over the same epochs. The response of the fluid-transport and mechanical systems must be represented in a coherent manner to enable co-inversion of the efflux and geodetic data. As shown in **Fig. S1,** we consider an idealized magmatic system for SHV, which is arguably typical of many other andesitic volcanoes worldwide. The system contains separate deep and shallow magmatic chambers, arrayed vertically, and connected by intervening conduits.

Fluid-transport system: Vertical conduits connect the two reservoirs, and link the system to both the mantle and the surface. The magma charges the upper (I) and lower (II) reservoirs at mass rates $\frac{d}{dt}(\rho V)^I$ and $\frac{d}{dt}(\rho V)^{II}$, respectively, via the adjoining conduits where ρ is average magma density and V^i is the volume of chamber i. The conduits have little capacity for magma storage, relative to the reservoirs, and storage within the conduits is neglected. The linking conduits are of small diameter (~30 m); at this dimension the surface geodetic response is insensitive to their effect at the wide aperture (>3 km) considered here. Mass is conserved within the flowing system where the mass rate of change of chamber i may be linked to the magma mass influx (ρq^i_{in}) and efflux (ρq^i_{out}), where q^i_{in} is the volume rate, as $\frac{d}{dt}(\rho V)^i = \rho q^i_{in} - \rho q^i_{out}$.

The independent effect of magma expansion by decompression ($\dot{\rho}$), and the volume change of the chamber ($\dot{V}$), apparent in the geodetic signal may be separated as,

---

[1] College of Earth and Mineral Sciences, Penn State University, University Park, PA 16802, USA. +1.814.865.2225 (Vx); +1.814.865.3248 (Fx); elsworth@psu.edu

[2] Department of Geosciences, University of Arkansas, Fayetteville, AR 72701, USA

[3] School of Environmental Sciences, University of East Anglia, Norwich, NR4 7TJ, UK

$$\frac{d}{dt}(\rho V)^i = V^i\dot{\rho} + \rho\dot{V}^i = \rho q_{in}^i - \rho q_{out}^i \,. \tag{1}$$

The rate of change in magma density ($\dot{\rho}$) is related to the bulk modulus of the magma (K_M) as,

$$\dot{\rho} = \frac{\rho}{K_M}\,\dot{p} \tag{2}$$

through the rate of change in pressure ($\dot{p}$) and may be related to the volume change of a spherical chamber of radius a embedded in an elastic medium of shear modulus G_R as

$$\dot{V}^i = \frac{\pi a^3}{G_R}\,\dot{p} = \frac{3}{4}\frac{V^i}{G_R}\,\dot{p}\ . \tag{3}$$

Substituting the magma-pressure to chamber-volume relation of (3) to be congruent with the density change in the magma of equation (2), and the result into eqiation (1) yields

$$\rho(\frac{4}{3}\frac{G_R}{K_M} + 1)\dot{V}^i = \rho q_{in}^i - \rho q_{out}^i \,. \tag{4}$$

Further defining outputs from the system in terms of volume rates, q , defined at mean chamber density yields

$$\underbrace{(\frac{4}{3}\frac{G_R}{K_M} + 1)}_{C^i}\dot{V}^i = C^i\dot{V}^i = q_{in}^i - q_{out}^i \tag{5}$$

with the influence of magma compressibility represented in the multiplier, C^i and with volume fluxes defined in terms of dense rock equivalents (DRE). When the geodetically observed volume change of the chamber is equivalent to the volume change in the magma, when $C^i \to 1$, and the magma can be considered incompressible. Conversely, when $C^i > 1$, the volume change of the magma is greater than the volume change in the chamber alone, due to the finite compressibility of the magma. Therefore, the influence of magma compressibility on the resulting efflux is indexed relative to the ratios of the relative stiffnesses of the rock and magma (G_R / K_M) as embodied in the parameter C^i .

Assuming that there is no storage in the linking conduits, then for the twin chamber system considered here, $q_{in}^I = q_{out}^{II}$, enabling the relations

$$\begin{aligned} C^I\dot{V}^I &= q_{in}^I - q_{out}^I \\ C^{II}\dot{V}^{II} &= q_{in}^{II} - q_{out}^{II} \end{aligned} \tag{6}$$

to be combined as

$$C^I\dot{V}^I + C^{II}\dot{V}^{II} = q_{in}^{II} - q_{out}^I \tag{7}$$

where q_{out}^I is the observable surface efflux from the system recorded in DRE.

Mechanical system: Deformations result at the surface from the superposed inflation, or deflation, of both reservoirs. For an elastic system, with an inflating source at I, the radial ($\dot{r}_i$) and vertical ($\dot{z}_i$) surface velocities measured at some location ($r_i^I; R_i^I$: **Fig. S1**) are proportional to the reservoir inflation rate as $\dot{r}_i = a_i^I\dot{V}^I$ or $\dot{z}_i = b_i^I\dot{V}^I$. The terms a_i^I and b_i^I are coefficients relating to the disposition of the measuring point ($r_i^I; R_i^I$) relative to the source. The effect of multiple reservoirs may be accommodated by superposition of velocities. For the two-reservoir system considered here, the resulting radial velocities measured at locations $i = 1,2$ are,

$$\begin{aligned} \dot{r}_1 &= a_1^I\dot{V}^I + a_1^{II}\dot{V}^{II} \\ \dot{r}_2 &= a_2^I\dot{V}^I + a_2^{II}\dot{V}^{II}. \end{aligned} \tag{8}$$

where the coefficients linking the surface velocities to inflation rates are recovered from the Mogi solutions for a strain nucleus as $a_i^I = (3\ /\ 4\pi)(r_i^I\ /\ (R_i^I)^3)$ (*1, 2*). This represents the effect of an inflating chamber collapsed to a point within a homogeneous elastic half-space bounded by a horizontal surface, and for a Poisson ratio of $\upsilon = 0.25$. These assumptions have proved adequate for more restrictive analyses on the same system (*3*), and are used directly here.

The resulting surface radial velocities may be determined for a second reservoir (a_i^{II}) by permuting the coordinates ($r_i^{II}; R_i^{II}$). Alternately, if vertical displacement rates are available then the equivalent of equation (8) may be constructed with $\dot{z}_i = b_i^I\dot{V}^I$ and $b_i^I = -(3\ /\ 4\pi)(z_i^I\ /\ (R_i^I)^3)$.

Co-Inversion: Velocities measured at two different radial distances (say radial velocities $\dot{r}_1$ *and* $\dot{r}_2$) together with the surface efflux (q_{out}^I) enable equations (7) and (8) to be solved simultaneously for the two reservoir inflation rates $\dot{V}^I$ and $\dot{V}^{II}$, and the supply to the deep crust/mantle flux q_{in}^{II}. From these, the full suite of flux terms defining exchange between the various reservoirs may be determined. Importantly, measured velocities must be available at two different radial locations – radial and vertical velocities measured at a single location are not independent – although, vertical and radial velocities from different locations may be mixed. In this discussion, the depths and locations of the reservoirs are assumed known, but are based on inversions of the entire surface deformation field at specific epochs (*4, 5*). If additional reservoirs

are present, the number of displacement measurements required increments for each additional reservoir.

Analysis of cGPS Data: The idealized geometry of the magmatic plumbing system is shown in **Fig. S1**. Magma efflux rate and episodic removal by dome failure has been recorded continuously since the inception of the eruption in 1995 (*6-8*). Similarly, long-term surface displacements have been recorded since 1995 by cGPS stations 3-8 km from the conduit and at a full range of azimuths, as shown in **Fig. 1** (*4, 5*). All GPS data were processed as absolute point positions using procedures similar to those reported elsewhere (*9*). Of these stations, only four have continuous records of displacements throughout the entire period of the eruption, and are thus suitable in this analysis to determine long-term trends in magma supply and exchange within storage volumes the crust. In order of increasing distance from the conduit, these stations are WYTD (2.8 km), SOUF (3.2 km), HARR (3.4 km), MVO1 (7.4 km) (**Fig. S1)** with histories of magma efflux (DRE) and station velocities reported in **Table S1** and plotted in **Fig. 2**. Data are divided into three separate cycles, each containing an eruptive episode followed by a pause. These eruptive episodes and pauses are later used to categorize characteristic features of the magma transport history.

To maximize the sensitivity of the analysis to processes at depth, the Caribbean-fixed velocity (*10*) (radial) and vertical velocity relative to the Earth's barycenter of the widest aperture station (MVO1) is combined with the velocity of each of the closer stations in three paired combinations. The average of these three independent evaluations of magma transfer rate is shown in **Fig. 3,** together with error bars, where the magma is assumed incompressible ($C^I = C^{II} = 1$). Apparent from these are: (1) the relatively small variation in calculated magnitudes of magma supply between the geodetic data from the three paired stations; and (2) the relative consistency between inflation-deflation and magma exchange in each eruptive episode, and pause. These observations allow us to infer that the three separate episodes are products of a nearly invariant plumbing system.

Influence of Magma Compressibility: Where the magma is slightly compressible ($C^i > 1$), the volume change of magma within the chamber will be larger than the geodetically recorded volume-change signal. This severity of this effect is indexed relative to the ratios of wall-rock to magma stiffness (reciprocal compressibility) (G_R / K_M).

The **shear modulus of the wall rock** may be indexed relative to p-wave magnitudes which vary between ~3 km/s at sea level beneath the volcano to ~6 km/s at 6-12 km. The small strain shear moduli estimated from these (Poisson ratio of 0.25) range between 5 and 10 GPa. Large

strain moduli may be an order of magnitude lower in representing the larger displacements accommodated in the long-term inflationary and deflationary response(*3, 11*). Shallow to intermediate depth shear moduli are estimated in the range 1-5 GPa from surface tilt data (*3*). The lower end of this range is congruent with stress drops anticipated during deflation, expected to be of the order of 1-10 MPa. From $dV \sim (V \,/\, G_R)dp$ [Equation (3)] the pressure drop for the evacuation of ~150 Mm^3 from the lower chamber (**Fig. 4**) is in the range 250-25 MPa for chamber volumes in the range 1-10 km^3 for a shear modulus of $G_R = 5$ MPa. A shear modulus of *5* GPa is considered the upper limit of the applicable range for SHV.

The **compressibility of the magma**, and its reciprocal bulk modulus (K_M) varies significantly with exsolved gas fraction (*12*). For water contents of the primitive magmas of the order of 6 wt% (*13, 14*) and for an upper limit of crystals above the percolation threshold (*15*) of the order of 40%, this results in bulk moduli of the order of 1.9 GPa at 6 km and 42.6 GPa at 12 km ($800°C$ and bulk modulus of the melt and crystals of 10 GPa). Thus, for wall rock shear moduli in the range $G_R = 1 - 5$ GPa, the compressibility factors, C^i are in the ranges 1.7-4.5 at 6 km and 1.03-1.16 at 12 km. The influence of these magnitudes on the resulting distribution of magma transfer is shown in **Fig. S1** for incompressible through compressible magmas with $G_R = 0, 1, 5$ GPa. The corresponding influence of magma compressibility on the volumetric inflation rates in the upper and the lower chamber are shown in **Fig. S3**. Apparent from the response is that for the depths selected here, the magma may be considered incompressible relative to the surrounding host rock.

Temporal Volume Change for a Deflating Spherical Reservoir: Cumulative volume change with time $dV(t)$, for a spherical reservoir discharging through a constant diameter conduit may be defined in terms of the total volume change dV_T, the compliance of the combined magma and chamber system, $\tilde{C}$, and the Poisseiulle resistance of discharge along the conduit B as

$$dV(t) = (\tilde{C}\ dP_T)\exp(\frac{-Bt}{\tilde{C}}) = (dV_T)\exp(\frac{-Bt}{\tilde{C}})\,. \qquad (9)$$

The compliance of the chamber is given as $\tilde{C}^i = \pi a^3\left(\frac{1}{G_R} + \frac{4}{3}\frac{1}{K_M}\right) = \frac{\pi a^3}{G_R}C^i$ where behavior is modulated by the shear modulus of the rock surrounding the chamber G_R, the bulk modulus of the magma K_M and the radius of the chamber a. Magma of viscosity μ_M discharges through a conduit of radius $b\,(15m)$, length $h\,(12km)$ as $B = \frac{\pi d^4}{8h\mu_M}$. Parameter magnitudes are applied as

given in **Table S2**, enabling the change in chamber volume to be followed with time, as shown in **Fig. 4**.

References

1. D. F. McTigue, *Journal of Geophysical Research-Solid Earth and Planets* **92**, 12931 (Nov 10, 1987).
2. K. Mogi, *Bull. of the Earthquake Research Institute* **36**, 99 (1958).
3. C. Widiwijayanti, A. Clarke, D. Elsworth, B. Voight, *Geophysical Research Letters* **32** (Jun 15, 2005).
4. G. S. Mattioli *et al.*, *Geophysical Research Letters* **25**, 3417 (Sep 15, 1998).
5. G. S. Mattioli, R. Herd, *Seismological Research Letters* **74**, 230 (2003).
6. Montserrat Volcano Observatory. Unpublished Data. (1995-2008).
7. J. D. Devine *et al.*, *Geophysical Research Letters* **25**, 3669 (Oct 1, 1998).
8. R. S. J. Sparks *et al.*, *Geophysical Research Letters* **25**, 3421 (Sep 15, 1998).
9. P. E. Jansma, G. S. Mattioli, *Geological Society of America Special Paper* **385**, 13 (2005).
10. C. DeMets *et al.*, *Geological Society of America Special Paper* **428**, 21 (2007).
11. B. Voight *et al.*, *Geophysical Research Letters* **33** (Feb 10, 2006).
12. H. E. Huppert, A. W. Woods, *Nature* **420**, 493 (Dec 5, 2002).
13. I. S. E. Carmichael, *American Mineralogist* **89**, 1438 (Oct, 2004).
14. M. Pichavant, R. Macdonald, *Contributions to Mineralogy and Petrology* **154**, 535 (Nov, 2007).
15. N. Petford, *Annual Review of Earth and Planetary Sciences* **31**, 399 (2003).

List of Tables

		MVO1		HARR		SOUF		WYTD		
		7.38 km		3.38 km		3.22 km		2.85 km		
Period	Dates	$\dot{r}$	$\dot{z}$	$\dot{r}$	$\dot{z}$	$\dot{r}$	$\dot{z}$	$\dot{r}$	$\dot{z}$	Efflux (m^3/s)
Episode 1	15 Nov 1995 – 10 Mar 1998	N/A*	N/A	-6.51	-57.00	N/A	N/A	8.30	-68.50	4.1
Pause 1	10 Mar 1998 – 28 Nov 1999	12.06	10.10	6.33	30.90	7.06	-7.20	11.85	27.80	0.06
Episode 2	28 Nov 1999 – 31 July 2003	-19.92	-32.10	-14.71	-27.30	-10.59	-29.50	3.05	-45.30	2.25
Pause 2	31 July 2003 – 1 Aug 2005	16.33	23.00	11.01	28.80	8.98	17.70	6.39	29.60	0.02
Episode 3	1 Aug 2005 – 4 April 2007	-41.60	-47.70	-33.04	-89.00	-23.35	-31.50	-28.91	-81.10	6.0
Pause 3	4 April 2007 – Dec 2008	19.15	6.40	0.922	46.00	10.06	16.00	-8.71	53.20	0.0

		LKYN		RDIO		STGH		REID		ROCH		
		8.81 km		3.91 km		3.52 km		3.46 km		2.81 km		
Period	Dates	$\dot{r}$	$\dot{z}$	$\dot{r}$	$\dot{z}$	$\dot{r}$	$\dot{z}$	$\dot{r}$	$\dot{z}$	$\dot{r}$	$\dot{z}$	Efflux (m^3/s)
Episode 1	15 Nov 1995 – 10 Mar 1998	-30.5	-33.4	-15.9	-55.2	-19.4	-43.1	-8.3	-44.4	-3.8	-71.8	4.1

*N/A=Not Available

Table S1: Dense rock equivalent (DRE) efflux rates and average radial and vertical station velocities measured over the three episodes of activity-followed-by-repose for the four stations used in the analysis. Velocities in mm/y. Calculations are for chambers centered at depths of 6 km and 12 km.

Parameter	Symbol	Assigned Value
Chamber Radius	a	1000 m
Conduit Radius	R	15 m
Chamber Depth	h	12,000 m
Shear Modulus of Host Rock	G_R	3 GPa
Bulk Modulus of Magma	K_M	1.1 GPa
Magma Viscosity	μ_M	5.5×10^7 Pa·s
Total Chamber Volume Change[a]	dV_T	338 Mm^3

Three values of final volume change are used to generate the range (shadow) of exponential curves in **Error! Reference source not found.**4. 308, 338, and 368 Mm^3 [a]Total chamber volume change is for the completing eruptive cycle, until pressure drive stalls.

Table S2: Parameters used to represent cavity deflation for chambers at 6 km and 12 km.

List of Figures

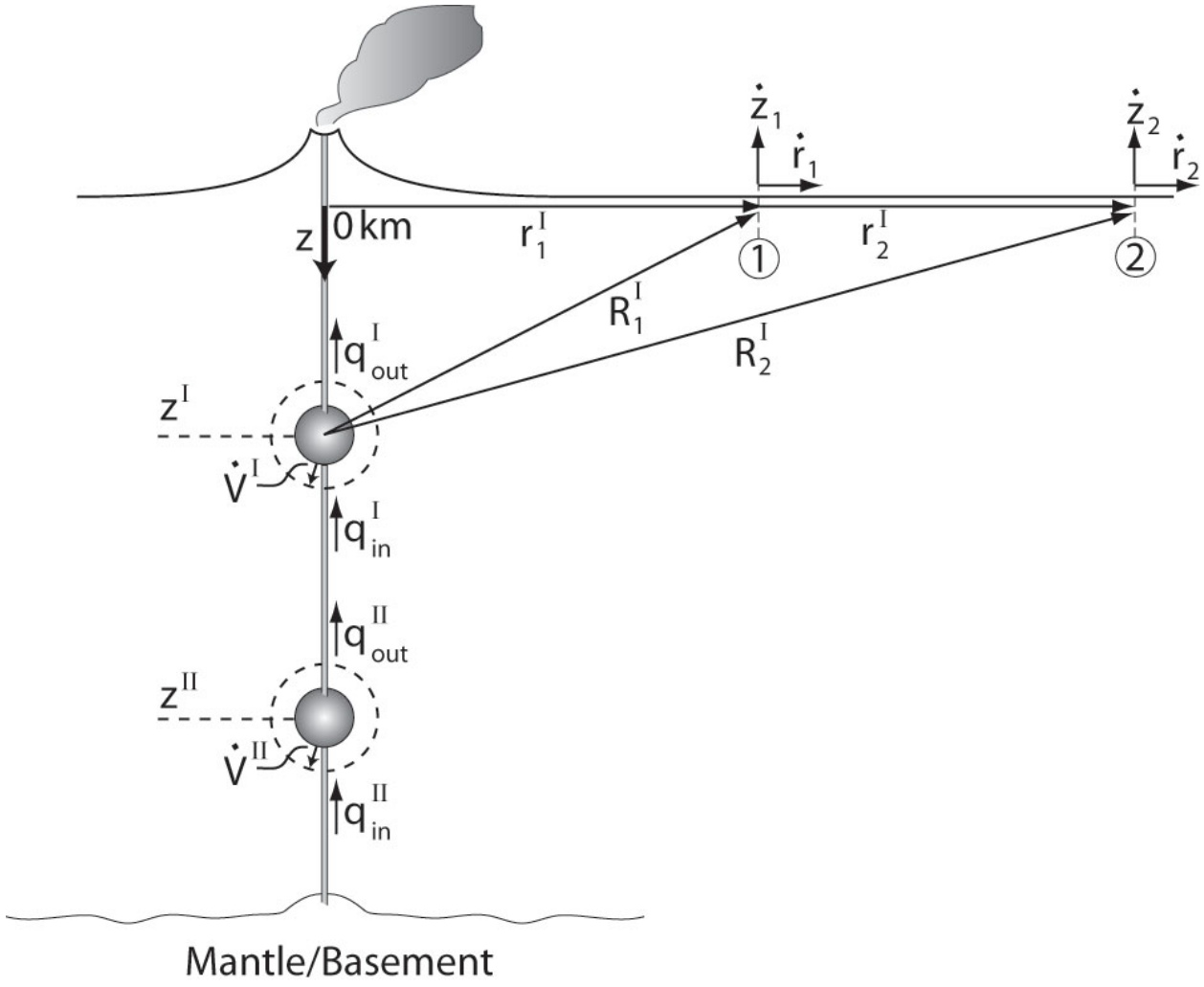

Fig. S1: Schematic of the magmatic plumbing system considered here. Adjacent reservoirs I and II are linked by conduits with little magma volume or storage. Inflating reservoir I at volumetric rate $\dot{V}^I$ results in surface displacement rates in the radial $\dot{r}_1^I$ and vertical $\dot{z}_1^I$ measured at location $(r_i^I; R_i^I)$.

(A)

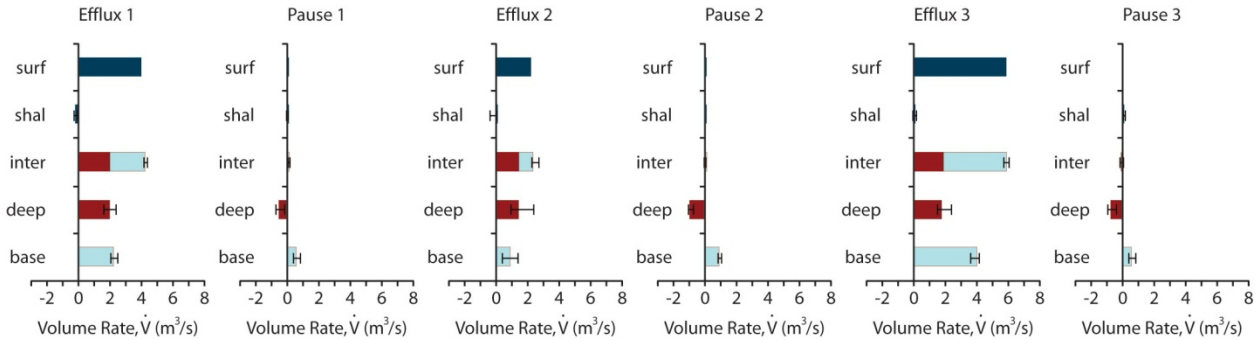

(B)

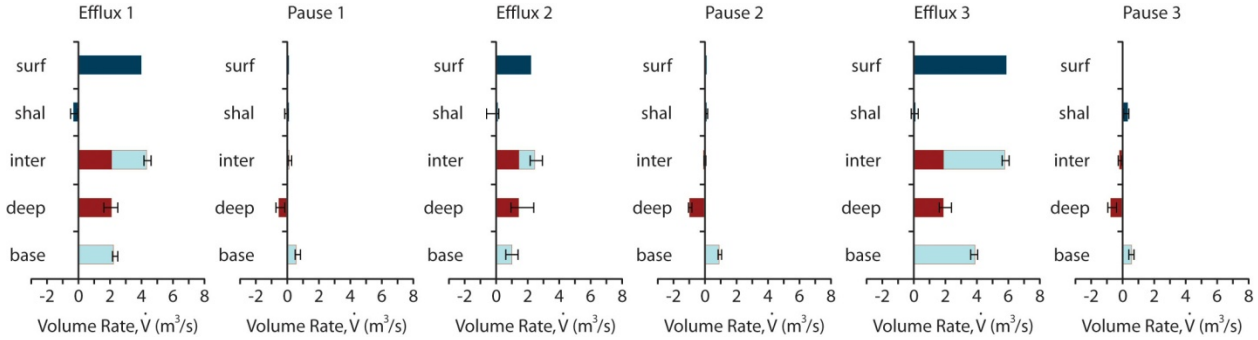

(C)

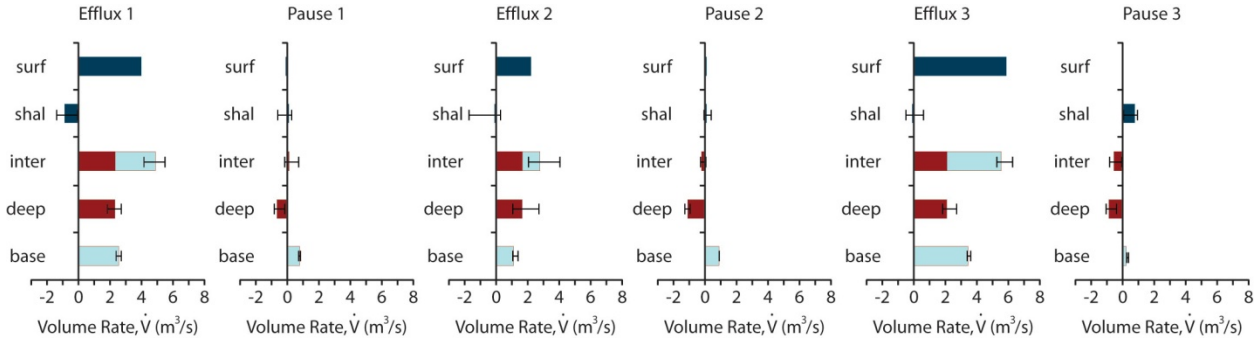

Fig. S2: Average inter-chamber, basement supply, and chamber inflation rates recovered from co-inversion of surface efflux and geodetic data for dual chamber geometry as in Figure 3. Results are for shear modulus of wall rock of (A) $G_R = 0\ GPa$ (incompressible as shown in Figure 3(A), (B) $G_R = 1\ GPa$ and (C) $G_R = 5\ GPa$. Flux rates are in $m^3\ /\ s$ of dense rock equivalent (DRE) with surface efflux measured and all others calculated.

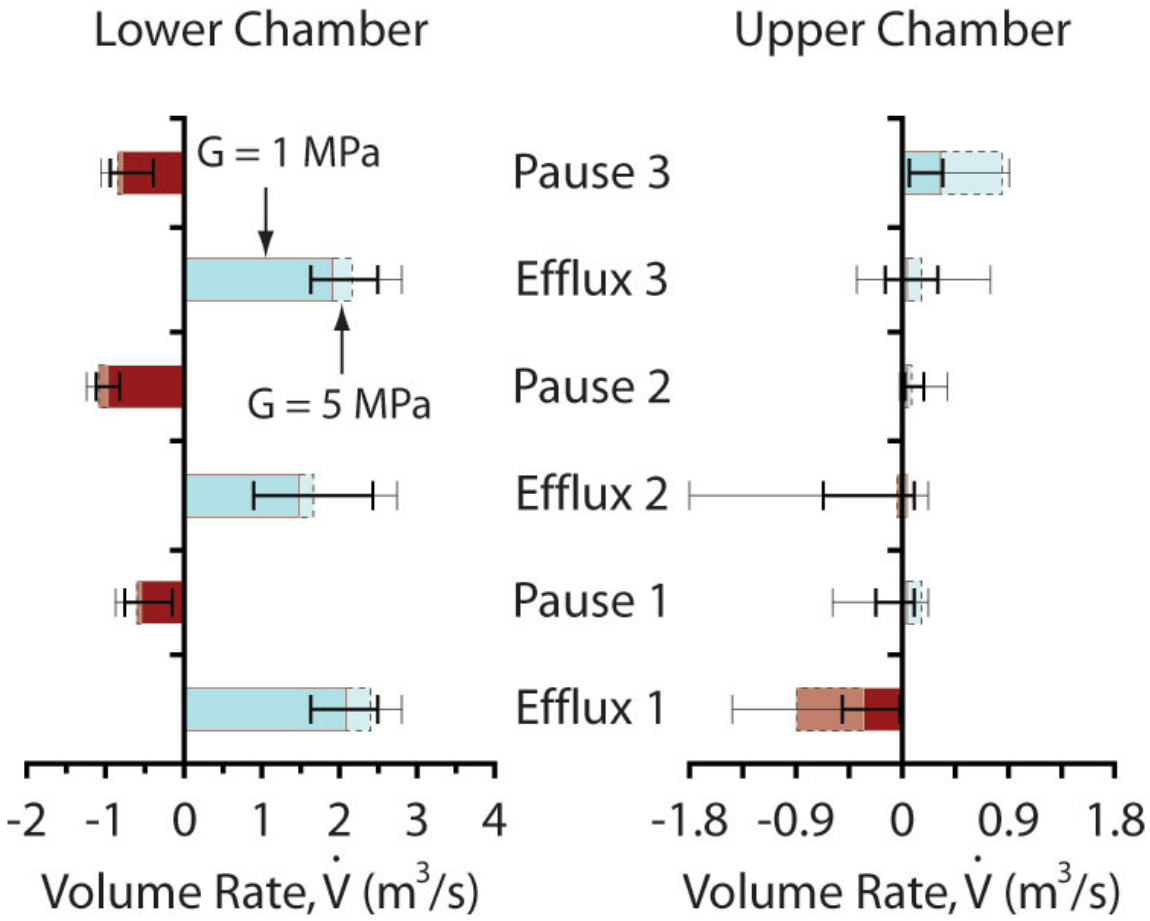

Fig. S3: Volumetric deflation (positive) and inflation (negative) rates of the deep (lower) and shallow (upper) chambers for shear moduli G_R of the host rock of 1 (solid) and 5 GPa (transparent).